Volume 10
Number 40
28 October 2022
Pages 14781–15210

Journal of Materials Chemistry C

Materials for optical, magnetic and electronic devices

rsc.li/materials-c

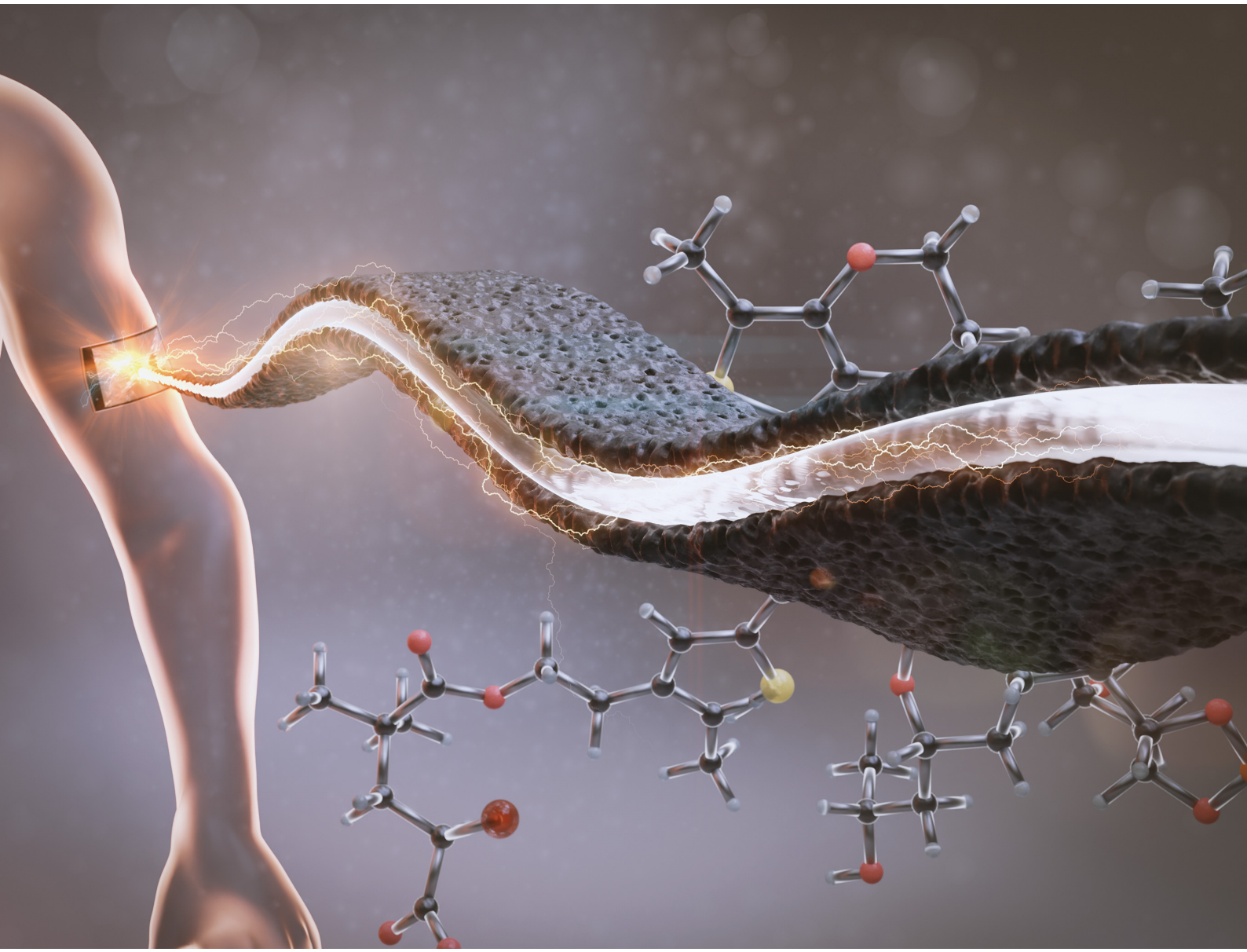

ISSN 2050-7526

ROYAL SOCIETY OF CHEMISTRY

PAPER

Bicheng Zhu, Jadranka Travas-Sejdic *et al.*
Soft, flexible and self-healable supramolecular conducting polymer-based hydrogel electrodes for flexible supercapacitors

Journal of Materials Chemistry C

ROYAL SOCIETY OF CHEMISTRY

PAPER

View Article Online
View Journal | View Issue

Cite this: J. Mater. Chem. C, 2022, 10, 14882

Soft, flexible and self-healable supramolecular conducting polymer-based hydrogel electrodes for flexible supercapacitors†

Bicheng Zhu,*[ab] Eddie Wai Chi Chan,[ab] Sheung Yin Li,[ab] Xin Sun[ab] and Jadranka Travas-Sejdic *[ab]

Conducting polymer-based hydrogels have drawn great attention recently as stretchable and soft electrode materials for flexible supercapacitors, for wearable electronics applications. In this work, we strategically combined a supramolecular approach and the ARGET–ATRP grafting methodology to prepare stretchable and self-healable poly(3,4-ethylenedioxythiophene) (PEDOT)-based conductive hydrogels with excellent electrochemical and mechanical properties. The supramolecular assembly of thiophene-3-boronic acid (ThBA) and poly(vinyl alcohol) (PVA), *via* dynamic boronate bonds, provides robustness for the PEDOT-based hydrogel. The hydrogen bonds between poly(acrylic acid) (PAA)-grafted-thiophene and PVA offer the fast self-healing properties to the hydrogel when exposed to mild pressures. After integrating the PAA-grafted-thiophene/PVA-based hydrogel with the self-healable, borate ester cross-linked PVA hydrogel electrolyte, the formed supercapacitor structure exhibits a specific capacitance of 222.32 mF cm^{-2}, with an energy density of 19.8 μW h cm^{-2}. The PEDOT-based hydrogel exhibits excellent electrochemical stability with 95.8% capacitance retention after 1000 charging–discharging cycles and a good capacitance recovery rate of 78.3% after the cutting–healing cycle. The utilisation of a supramolecular approach and the ARGET–ATRP grafting methodology could guide future developments in intrinsically stretchable and self-healable materials for wearable bioelectronics. The developed, intrinsically flexible and self-healable energy-storage device has potential for applications in the next generation of epidermal bioelectronics or other wearable electronics devices.

Received 2nd August 2022,
Accepted 20th September 2022

DOI: 10.1039/d2tc03239b

rsc.li/materials-c

Introduction

The current developments in flexible biosensors and bioelectronics pay increasingly more attention to developing soft materials for wearable, epidermal and implantable devices.[1,2] The power supply sources, such as batteries and supercapacitors, for these soft devices also need to be flexible and soft, as they are required to work under various mechanical deformations alongside the rest of the bioelectronics components.

Conducting polymer-based soft materials are promising candidates to be utilised as soft and flexible electrodes in bioelectronics applications, due to their ease of synthesis, soft mechanical properties, good conductivity, environmental stability and high pseudocapacitance.[3–6] To alter the rigid nature of conducting polymers into stretchable and flexible formats, molecular engineering has been investigated, where soft side chains have been grafted onto the rigid conducting polymer backbone.[2] The hydrogel format of conducting polymer-based materials has also been investigated to overcome the stiffness and non-flexible nature of the conducting polymers.[7,8] Poly(vinyl alcohol) (PVA) has been widely applied as a soft matrix that incorporates well with the rigid conducting polymers. It is amenable to crosslinking using both physical[9] and chemical methodologies.[10,11] Li *et al.* recently incorporated bis(trifluoromethane)sulfonamide lithium salt (LiTFSI) into a PEDOT:PSS and poly(vinyl alcohol) (PVA) hydrogel, which produced a supercapacitor with an areal capacitance of 44.5 mF cm^{-2} and a power density of 0.04 mW cm^{-2}.[12] Sun *et al.* demonstrated an 'all-in-one supercapacitor' that was fabricated with two embedded polypyrrole (PPy) layers as electrodes and the boron cross-linked PVA/KCl hydrogel film as a solid-state electrolyte.[11] The all-in-one supercapacitor showed superior toughness and mechanical strength when exposed to large deformations, with an areal capacitance of 224 mF cm^{-2} and an energy density of 20 μW h cm^{-2} under deformation.

[a] Polymer Biointerface Centre, School of Chemical Sciences, The University of Auckland, Auckland 1010, New Zealand. E-mail: bicheng.zhu@auckland.ac.nz, j.travas-sejdic@auckland.ac.nz
[b] MacDiarmid Institute for Advanced Materials and Nanotechnology, Wellington, New Zealand

† Electronic supplementary information (ESI) available. See DOI: https://doi.org/10.1039/d2tc03239b

To further improve the robustness and the mechanical performance of the conducting polymer-based hydrogel for epidermal bioelectronics, the supramolecular crosslinking strategies between rigid conducting polymers and soft polymers have been investigated.[13–17] Li *et al.* reported a high performance, flexible, solid-state supercapacitor based on the supramolecular assembly of polyaniline (PANI) and polyvinyl alcohol (PVA), made through boronate bonds.[14] The developed supercapacitor exhibited a specific capacitance of 153 F g^{-1}, with a high energy density of 13.6 W h kg^{-1}. Chen *et al.* developed boronate cross-linked PEDOT, which showed a high energy density of 15.2 W h kg^{-1} and a power density of 201.1 W kg^{-1}.[15]

Self-healing is one of the most important requirements for soft epidermal and implantable bioelectronics devices, including energy storage devices, as the performance should be retained after damage to the device.[18] To make a supercapacitor self-healable, either the electrolyte or the electrodes, or both, could be designed to be self-healable. Huang *et al.* reported a poly(acrylic acid) (PAA)-based electrolyte, dual crosslinked by hydrogen bonding between carboxylic acid groups and silica-based nanoparticles, which provided the intrinsic self-healability and high stretchability to the supercapacitor.[19] Han *et al.* demonstrated a poly(vinyl alcohol-borax) (PVAB) hydrogel and carbon nanotube–cellulose nanofiber (CNT–CNF) nanohybrids, displaying a specific capacitance of 117.1 F g^{-1} and a high capacitance retention ($\sim$98.2%) after ten damaging/self-healing cycles.[20] Yang *et al.* developed a supramolecular poly(vinyl alcohol)/poly(*N*-hydroxyethyl acrylamide) (PVA/PHEA) hydrogel electrolyte, which was decorated by chemically polymerised polyaniline (PANI) on two sides of the PVA/PHEA hydrogel electrolyte, forming an all-in-one supercapacitor device. The developed device was reported to exhibit a specific capacitance of 98 mF cm^{-2}.[21]

In this work, we developed a soft and flexible conducting polymer-based supercapacitor device using a copolymer of poly(acrylic acid)-grafted-thiophene (Th-*g*-PAA), 3,4-ethylenedioxythiophene (EDOT) and thiophene-3-boronic acid (ThBA). The rigid conducting polymer and the soft poly(vinyl alcohol) (PVA) then self-assembled through supramolecular interactions between the boronic acid groups from thiophene-3-boronic acid and hydroxy groups from PVA. Such a supramolecular assembly strategy is expected to enhance the mechanical and electrochemical properties.[14,22] To the best of our knowledge, this is the first report on utilising a supramolecular assembly strategy and the ARGET (activators regenerated by electron transfer)–ATRP (atom transfer radical polymerization) grafting methodology for the development of flexible, self-healable supercapacitor devices with the desired properties of stretchability, self-healing and robustness. The assembled soft electrodes exhibited a specific capacitance of 335.40 $\pm$ 4.61 mF cm^{-2} at a scan rate of 10 mV s^{-1}. In addition, the carboxylic acid groups from PAA-grafted-thiophene form hydrogen bonds with hydroxyl groups from PVA, offering rapid self-healing properties.[19] The self-healing occurs within 15 min at room temperature upon applying mild pressure. The poly(EDOT-*co*-(Th-*g*-PAA)-*co*-ThBA)–PVA hydrogel was integrated with a self-healable, diol-borate ester crosslinked PVA hydrogel to obtain a "sandwich" structured supercapacitor. The integrated supercapacitor exhibited a specific capacitance of 222.32 $\pm$ 7.59 mF cm^{-2} at 10 mV s^{-1} with a maximum energy density of 19.8 μW h cm^{-2}. The whole integrated device is self-healable, as each component of the device is self-healable. The recovery rate of the device's capacitance, after a cutting–healing cycle, was found to be 78.3%.

Results and discussion

The schematic of the flexible, conducting polymer (CP) hydrogel-based supercapacitor is given in Fig. 1A. The chemical structure of the poly(EDOT-*co*-(Th-*g*-PAA)-*co*-ThBA)–PVA hydrogel electrodes is shown in Fig. 1B. To prepare poly(EDOT-*co*-(Th-*g*-PAA)-*co*-ThBA)–PVA hydrogel electrodes, thiophene was first grafted with poly(*tert*-butyl acrylate) (poly(*t*BA)) by means of ARGET–ATRP, followed by poly(*t*BA) hydrolysis that afforded Th-*g*-PAA (Fig. 1C). The three monomers, Th-*g*-PAA, ThBA and EDOT, were dissolved, along with PVA, in the mixed solvent of water and DMSO, and were polymerised by the addition of $FeCl_3$ and APS solution in water to form a poly(EDOT-*co*-(Th-*g*-PAA)-*co*-ThBA)–PVA hydrogel (Fig. 1B). Here, the binary oxidant of $FeCl_3$ and APS was used for chemical polymerisation, as APS has a higher polymerisation rate but a low solubility in DMSO, while also Cl^- from $FeCl_3$ could act as a dopant for the conducting polymer to enhance the conductivity.[23]

To achieve the optimum capacitance, the composition of the poly(EDOT-*co*-(Th-*g*-PAA)-*co*-ThBA)–PVA hydrogel electrode was optimised, where the utilisation of both EDOT and thiophene (Th) as spacer monomers was investigated. In Fig. 2A, the CV plots of poly(EDOT-*co*-(Th-*g*-PAA)-*co*-ThBA)–PVA and poly(Th-*co*-(Th-*g*-PAA)-*co*-ThBA)–PVA hydrogels are shown. Based on CV plots, the poly(EDOT-*co*-(Th-*g*-PAA)-*co*-ThBA)–PVA hydrogel exhibited a higher capacitance at 100 mV s^{-1} of 206.25 $\pm$ 5.75 mF cm^{-2} compared to 181.25 $\pm$ 6.89 mF cm^{-2} obtained from the poly(Th-*co*-(Th-*g*-PAA)-*co*-ThBA)–PVA hydrogel, as shown in Fig. 2B. Therefore, EDOT was chosen for further synthesis of hydrogel electrodes.

In the process of the preparation of a poly(EDOT-*co*-(Th-*g*-PAA)-*co*-ThBA)–PVA hydrogel, PSS was added to enhance the uniformity of the dispersion of the monomer and PVA mixture, as reported by Wei *et al.*,[24]. The CV measurements of the hydrogel electrodes at 100 mV s^{-1}, with and without the addition of PSS, are shown in Fig. 2C. The capacitance of the poly(EDOT-*co*-(Th-*g*-PAA)-*co*-ThBA)–PVA hydrogel prepared with PSS was 206.25 $\pm$ 5.75 mF cm^{-2} calculated from CV, compared to 81.57 $\pm$ 7.62 mF cm^{-2} obtained for the hydrogel prepared without PSS, as shown in Fig. 2D. Thus, as PSS indeed increased the capacitance of the prepared poly(EDOT-*co*-(Th-*g*-PAA)-*co*-ThBA)–PVA hydrogel, PSS was used in all subsequent experiments.

Characterisation of the poly(EDOT-*co*-(Th-*g*-PAA)-*co*-ThBA)–PVA hydrogel

The kinetics of the grafting of *t*BA onto ThBr was evaluated by employing 1H NMR, *via* tracking the consumption of the *t*BA

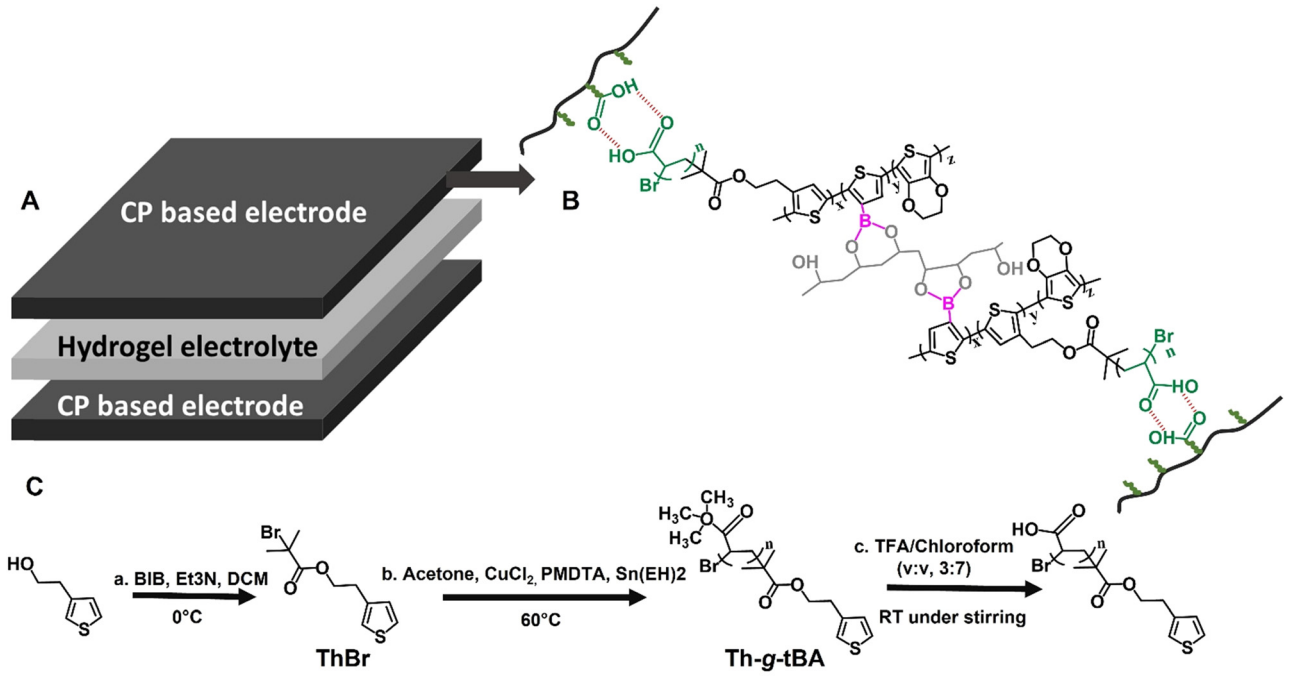

Fig. 1 (A) The "sandwich" structure of the supercapacitor. (B) The chemical structure of the poly(EDOT-*co*-(Th-*g*-PAA)-*co*-ThBA)–PVA hydrogel. (C) Synthetic route to Th-*g*-PAA.

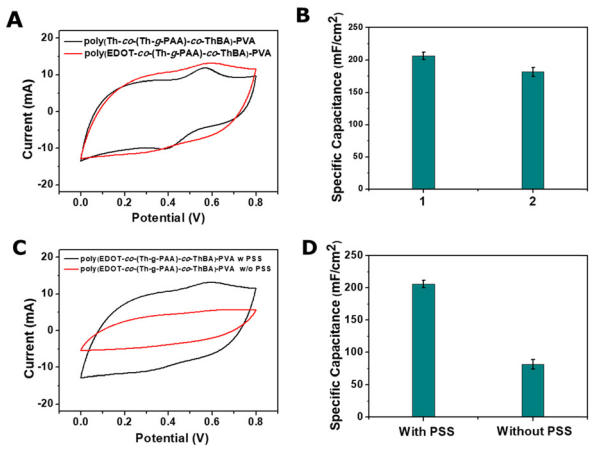

Fig. 2 (A) Cyclic voltammograms (CVs) and (B) areal specific capacitances of (1) poly(EDOT-*co*-(Th-*g*-PAA)-*co*-ThBA)–PVA hydrogels and (2) poly(Th-*co*-(Th-*g*-PAA)-*co*-ThBA)–PVA hydrogel electrodes in 2 M KCl solution at a scan rate of 100 mV s^{-1}. (C) CV and (D) areal specific capacitance of poly(EDOT-*co*-(Th-*g*-PAA)-*co*-ThBA)–PVA hydrogels with and without PSS.

monomer during the reaction. The kinetic plot for the polymerisation is presented in Fig. 3A. After 3 h reaction, the conversion of *t*BA reached 91%, giving the average number of repeat units for *t*BA per initiating site of about 14. The successful hydrolysis of Th-g-*t*BA into Th-*g*-PAA was confirmed by 1H NMR from the appearance of the peak at δ = 12.2 (--COOH) (Fig. 3B). The number of repeat units of PAA was estimated from the ratio of the peak at δ = 12.2 (–COOH) to the peak at δ = 6.98 (thiophene), revealing 14 repeat units of PAA, in agreement with the results for incorporated *t*BA units obtained from kinetic analysis.

The polymerisation of Th-*g*-PAA, ThBA and EDOT with $FeCl_3$ and APS turned the reaction mixture into dark green within 1 min of polymerisation, without any visible precipitation. It is considered that the physical and chemical crosslinks between CP and PVA chains render the formed polymer composite in a hydrogel state.[13] After the preparation process, the water content of the poly(EDOT-*co*-(Th-*g*-PAA)-*co*-ThBA)–PVA hydrogel was 86.3%.

The FT-IR spectra, as shown in Fig. 3C, of the poly(EDOT-*co*-(Th-*g*-PAA)-*co*-ThBA)–PVA hydrogel showed the characteristic absorption bands at around 652 cm^{-1} and 1315 cm^{-1}, corresponding to the bending of O–B–O[11] and the asymmetric stretching of B–O–C.[9] A comparison of the FTIR spectra of PVA and poly(EDOT-*co*-(Th-*g*-PAA)-*co*-ThBA)–PVA hydrogels reveals that the peak intensity of the –OH stretching vibration of PVA, in the range of 3200–3400 cm^{-1}, weakens after crosslinking with boronic acid groups. Moreover, to confirm the existence of the hydrogen bonds, a major adsorption band from PVA at 3429 cm^{-1} corresponds to the stretching of hydroxyl groups, which shifts to 3273 cm^{-1} due to the formation of hydrogen bonds, in agreement with the shift reported elsewhere.[25] XRD was applied to investigate the crystalline structure of the poly(EDOT-*co*-(Th-*g*-PAA)-*co*-ThBA)–PVA hydrogel. The XRD pattern of commercial PEDOT:PSS, shown in Fig. S2A (ESI†), shows a broad diffraction peak at 2θ of 25.5°, which was attributed to interchain planar ring-stacking.[26] By comparison, the XRD spectra of poly(EDOT-*co*-(Th-*g*-PAA)-*co*-ThBA)–PVA show a broad amorphous peak in the region from 2θ *ca.* 15 to 30° in which are superimposed somewhat sharper peaks at 25.5° and 19.9° that

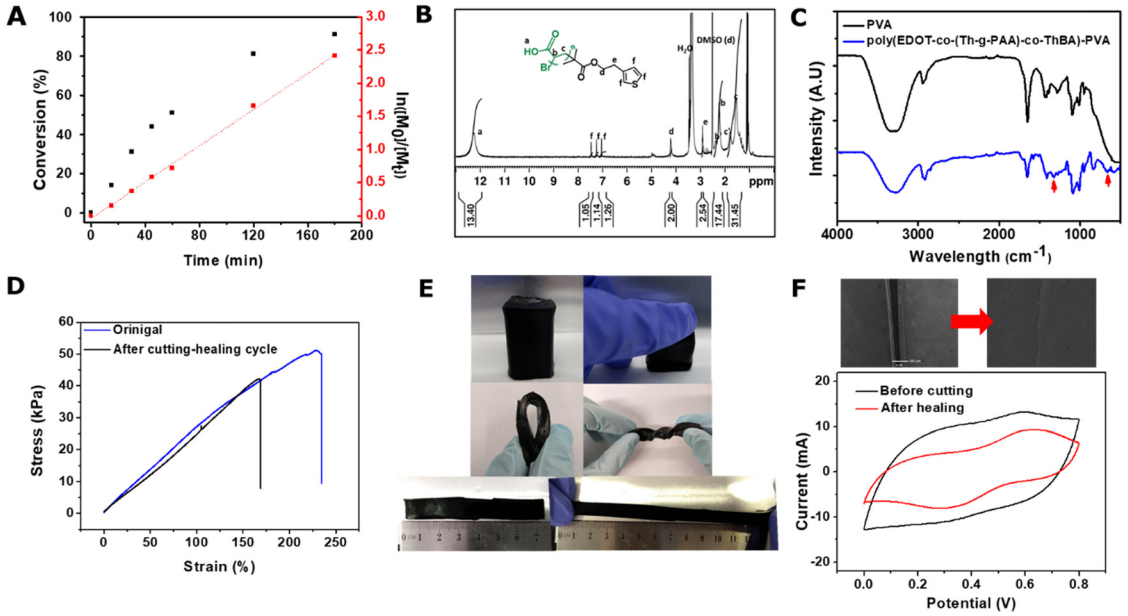

Fig. 3 (A) Kinetic plot of monomer conversion and $\ln([M_0]/[M_t])$ *vs.* time for the ATRP of *t*BA from ThBr. The dashed line represents the linear fit to the experimental data. (B) 1H NMR data of Th-*g*-PAA in $CDCl_3$. (C) FTIR spectra of the poly(EDOT-*co*-(Th-*g*-PAA)-*co*-ThBA)–PVA hydrogel and PVA hydrogel. (D) Tensile stress–strain curve of the poly(EDOT-*co*-(Th-*g*-PAA)-*co*-ThBA)–PVA hydrogel. (E) The optical photographs of poly(EDOT-*co*-(Th-*g*-PAA)-*co*-ThBA)–PVA and poly(EDOT-*co*-(Th-*g*-PAA)-*co*-ThBA)–PVA hydrogels under various mechanical deformations: compression, bending, twisting and stretching. (F) CV measurements and SEM images of the poly(EDOT-*co*-(Th-*g*-PAA)-*co*-ThBA)–PVA hydrogel electrode before and after the cutting–healing cycle.

correspond to the (020) plane for PEDOT[26] and (101) and (200) planes for PVA,[27] respectively. The Raman spectrum of poly(EDOT-*co*-(Th-*g*-PAA)-*co*-ThBA)–PVA is shown in Fig. S2B (ESI†). The peaks at 441 and 696 cm^{-1} correspond to the C–O–C and C–S–C deformations, while the peaks at 990 and 1260 cm^{-1} were assigned to the oxyethylene ring deformation and C_α–C_α inter-ring stretching. A significant symmetric C_α ═C_β stretching peak of poly(EDOT-*co*-(Th-*g*-PAA)-*co*-ThBA)–PVA appears at 1436 cm^{-1}, indicating the high length of conjugation in the conducting polymer chains, which confirms that the addition of PVA has a negligible effect on the polymerization process of poly(EDOT-*co*-(Th-*g*-PAA)-*co*-ThBA)–PVA and on its chain structure.[15] The SEM and TEM images of the freeze-dried poly(EDOT-*co*-(Th-*g*-PAA)-*co*-ThBA)–PVA hydrogel are presented in Fig. S1 (ESI†), showing a porous and continuous network of the hydrogel.

The overall performance of the flexible supercapacitors demands satisfactory mechanical strength under the practical operating conditions, including repetitive bending, folding and stretching. The mechanical characterisation was carried out, with the tensile test results displayed in Fig. 3D. The maximum tensile strength of the poly(EDOT-*co*-(Th-*g*-PAA)-*co*-ThBA)–PVA hydrogel was 51.21 ± 6.7 kPa and the elastic Young modulus of the hydrogel was 35.5 ± 4.3 kPa. These values fall within the range of soft biological tissues, such as muscles and tendons.[28] Moreover, as demonstrated in Fig. 3E, the poly(EDOT-*co*-(Th-*g*-PAA)-*co*-ThBA)–PVA hydrogel was able to resist various forms of deformations, including compression, stretching, twisting, bending and folding.

The self-healing ability of the composite hydrogel was investigated by measuring the CV before and after healing. The self-healing was achieved by spraying 100 μL of deionised water onto the hydrogel surface and applying about 1 kg cm^{-2} for 15 min. There was no obvious healing in the absence of deionised water and applying pressure, as these two parameters would facilitate the formation of the hydrogen bonds for self-healing.[25] The cut poly(EDOT-*co*-(Th-*g*-PAA)-*co*-ThBA)–PVA hydrogel self-healed well (Fig. 3F inset). Strain–stress tests and CVs (at 100 mV s^{-1}), before and after the cutting–healing cycle, are displayed in Fig. 3D and F. The maximum tensile strength of the healed poly(EDOT-*co*-(Th-*g*-PAA)-*co*-ThBA)–PVA hydrogel was reduced to 42.07 kPa, while the elastic Young modulus remained at a similar level of 33.7 kPa (Fig. 3D). As shown in Fig. 3F, the specific capacitance after the cutting and healing was 100.55 ± 6.54 mF cm^{-2}, compared with the original specific capacitance of 206.25 ± 5.75 mF cm^{-2}; therefore, 48.8 ± 1.8% of the specific capacitance was recovered. The recovery rate was comparable to, or better than, other reported self-healable supercapacitor electrodes. For example, Zou *et al.* reported polyaniline (PANI)–PVA hydrogel electrodes with dual physical cross-linking of 4-carboxyphenylboronic acid (CPBA) and calcium ions.[29] The recovered specific capacitance, after healing for 4 h, was about 35.0% of the original value.

Electrochemical performance of poly(EDOT-*co*-(Th-*g*-PAA)-*co*-ThBA)–PVA hydrogels as supercapacitor electrodes

To optimise the self-healing properties of the composite hydrogel, the effect of the length of side chains was investigated.

The CVs, in 2 M KCl at 100 mV s^{-1}, were recorded for poly(EDOT-*co*-(Th-*g*-PAA)-*co*-ThBA)–PVA hydrogels with various lengths of PAA chains. When the number of the repeating units in PAA was increased from 10 to 14, the capacitance of the poly(EDOT-*co*-(Th-*g*-PAA)-*co*-ThBA)–PVA hydrogel decreased slightly from 217.18 mF cm^{-2} to 206.25 ± 5.75 mF cm^{-2}. When the number of the repeating units in PAA increased further to 18 and 25, the capacitance, as calculated from CV measurements, significantly reduced to 139.06 mF cm^{-2} and 92.19 mF cm^{-2}, respectively, as shown in Fig. 4A. This can be expected, as the long side chains of PAA grafted from ThBr increase the total weight of the non-electrochemically active component in the composite, which in turn reduces the capacitance. Additionally, the shorter side chain from Th-*g*-PAA would induce a lower extent of hydrogen cross-linking between polymer chains, which may enable easier access of ions from the electrolyte, facilitating a higher capacitance.[30] The self-healing properties of poly(EDOT-*co*-(Th-*g*-PAA)-*co*-ThBA)–PVA hydrogels with 10 and 14 repeating units in PAA were compared. No obvious healing was observed in the poly(EDOT-*co*-(Th-*g*-PAA)-*co*-ThBA)–PVA hydrogel with 10 units, while the composite with 14 units in PAA showed a fast healing ability within 15 min, as shown in Fig. 3F. Hence, the poly(EDOT-*co*-(Th-*g*-PAA)-*co*-ThBA)–PVA hydrogel with 14 units is utilised for further study.

The amount of the Th-*g*-PAA in poly(EDOT-*co*-(Th-*g*-PAA)-*co*-ThBA)–PVA hydrogel was then optimised, where the amounts of EDOT and ThBA were kept constant. 2 μmol, 4 μmol and 8 μmol Th-*g*-PAA, corresponding to 2.4 mol%, 4.7 mol% and 9.5 mol% in the polymer composition, were investigated. The poly(EDOT-*co*-(Th-*g*-PAA)-*co*-ThBA)–PVA hydrogel with 4 μmol (4.7 mol%) Th-*g*-PAA

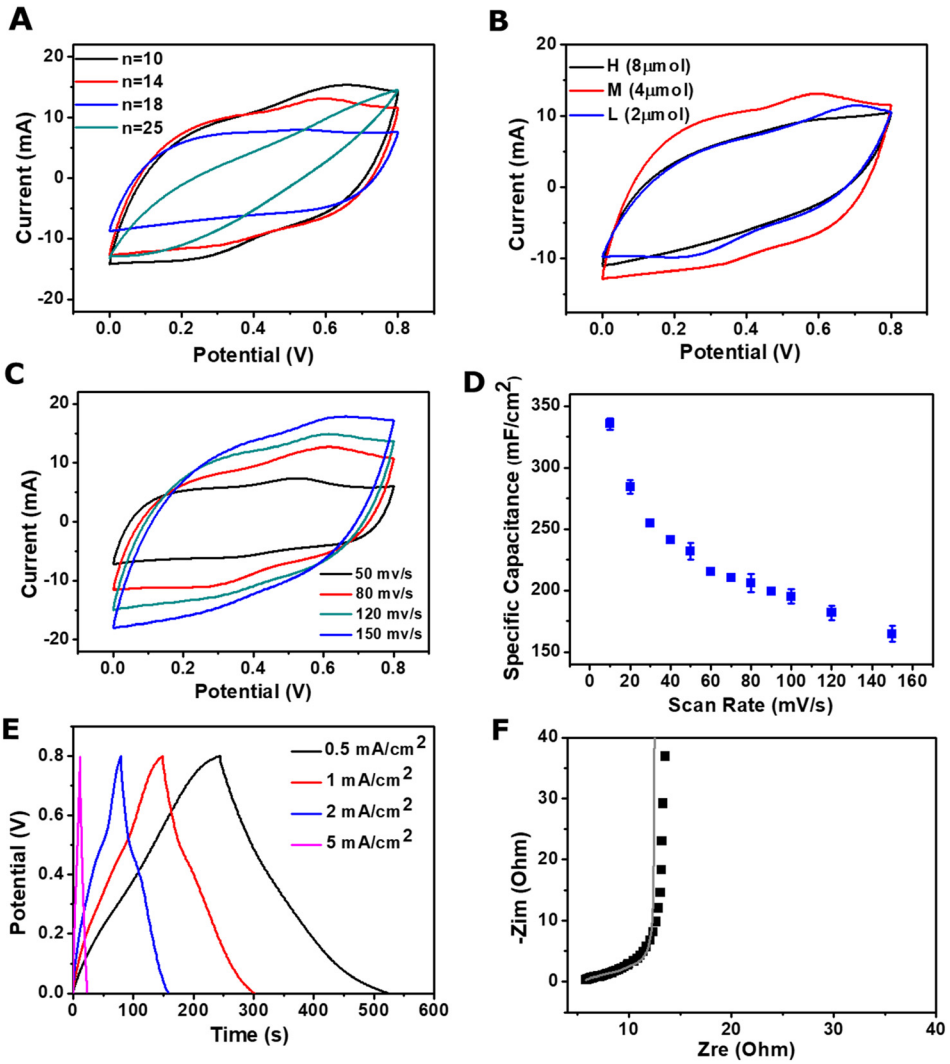

Fig. 4 CV measurements of poly(EDOT-*co*-(Th-*g*-PAA)-*co*-ThBA)–PVA hydrogels (A) with various lengths of PAA side chains and (B) with different molar fractions of Th-*g*-PAA. (C) Poly(EDOT-*co*-(Th-*g*-PAA)-*co*-ThBA)–PVA hydrogel (n of PAA in (Th-*g*-PAA) was 14, 4 μmol of (Th-*g*-PAA)) in 2 M KCl at different scan rates. (D) The specific capacitance of poly(EDOT-*co*-(Th-*g*-PAA)-*co*-ThBA)–PVA (n of PAA in (Th-*g*-PAA) was 14, 4 μmol (Th-*g*-PAA)) hydrogel electrodes at various scan rates in 2 M KCl solution. The error bars represent a standard deviation from 3 measurements. (E) GCD measurements for poly(EDOT-*co*-(Th-*g*-PAA)-*co*-ThBA)–PVA (n of PAA in (Th-*g*-PAA) was 14, 4 μmol (Th-*g*-PAA)) hydrogel electrodes at various current densities. (F) EIS spectra in the form of the Nyquist plot of poly(EDOT-*co*-(Th-*g*-PAA)-*co*-ThBA)–PVA (*n* of PAA in (Th-*g*-PAA) was 14, 4 μmol (Th-*g*-PAA)) hydrogels in the frequency range of 10 mHz to 100 kHz. The experimental data are shown as symbols and the fitted curves as solid lines.

exhibited an optimal specific capacitance of 206.25 mF cm^{-2}, compared with 132.81 mF cm^{-2} and 137.50 mF cm^{-2} for 8 μmol and 2 μmol, respectively, as estimated from the CVs presented in Fig. 4B. The increase in the amount of Th-*g*-PAA from 2 μmol to 4 μmol results in an increase in the specific capacitance due to the increase in the total amount of the electrochemically active polymer. When the amount of Th-*g*-PAA further increased to 8 μmol, a decrease in specific capacitance was observed, likely due to the inhibited access of the ions from the increased hydrogen bond cross-linking.[30] Therefore, 4 μmol Th-*g*-PAA was utilised for the preparation of poly(EDOT-*co*-(Th-*g*-PAA)-*co*-ThBA)–PVA hydrogel electrodes.

To explore the potential applications of the poly(EDOT-*co*-(Th-*g*-PAA)-*co*-ThBA)–PVA hydrogel for flexible supercapacitors, the hydrogel-based electrode was fabricated by using a carbon fibre cloth (CFC) as the current collector. In order to investigate the capacitance of the prepared poly(EDOT-*co*-(Th-*g*-PAA)-*co*-ThBA)–PVA hydrogel as an electrode on a CFC collector, CVs at different scan rates were performed in 2 M KCl electrolyte, as shown in Fig. 4C. From the CV measurements, the oxidation peak at 0.52 V and the reduction peak at 0.37 V were observed. The specific capacitance at different scan rates was calculated and is presented in Fig. 4D. The hydrogel electrodes exhibited a high areal specific capacitance of 335.40 ± 4.61 mF cm^{-2} at a low scan rate of 10 mV s^{-1}. The areal specific capacitance decreased when the scan rate increased, as expected, as at low scan rates the electrolyte ions would have time to diffuse in the bulk of the electrode, while at higher scan rates the electrolyte ion movement is limited to the surface layers of the electrode.[31] The GCD curves of the poly(EDOT-*co*-(Th-*g*-PAA)-*co*-ThBA)–PVA hydrogel, Fig. 4E, are nonlinear, which indicates the pseudocapacitive behaviour of the conducting polymer-based electrodes, in agreement with the CV results. The electrochemical resistance of the poly(EDOT-*co*-(Th-*g*-PAA)-*co*-ThBA)–PVA hydrogel–CFC electrode was examined by EIS, employing frequencies between 0.01 Hz and 100 kHz and open circuit bias potential, to obtain a detailed picture of the charge transfer and the electrochemical resistance. From the Nyquist plot (Fig. 4F), a negligible semicircle can be observed in the high-frequency region, indicating its low equivalent series resistance (R_s) of 4.62 Ω cm^{-2} and low charge transfer resistance (R_{ct}) of 2.56 Ω cm^{-2}, confirming the efficient charge-transfer kinetics of the poly(EDOT-*co*-(Th-*g*-PAA)-*co*-ThBA)–PVA hydrogel. Additionally, the nearly vertical slope of the plot in the low-frequency region indicates good capacitive behaviour of the electrode. These results suggest that the poly(EDOT-*co*-(Th-*g*-PAA)-*co*-ThBA)–PVA hydrogel electrode exhibits good electrochemical kinetics, ionic conductivity and good capacitance. The conductivity of the poly(EDOT-*co*-(Th-*g*-PAA)-*co*-ThBA)–PVA hydrogel was measured as 1 S cm^{-1}, using the setup shown in Fig. S3 (ESI†). This value was comparable with other conducting polymer-based hydrogels.[13,32]

Flexible supercapacitor performance

After optimisation of the composition of the poly(EDOT-*co*-(Th-*g*-PAA)-*co*-ThBA)–PVA hydrogel electrode, the hydrogel electrodes were integrated with a self-healable, PVA-based hydrogel electrolyte into a "sandwich" structured flexible supercapacitor. The PVA hydrogel was prepared based on other reports,[33,34] where the diol-borate ester bonding formed after mixing PVA and borax under alkaline conditions. The CV and GCD curves of the fabricated flexible supercapacitor were recorded to evaluate the electrochemical performance. There are redox peaks observed in the cyclic voltammogram of the device (Fig. 5A), which are in agreement with the voltammogram shape of the poly(EDOT-*co*-(Th-*g*-PAA)-*co*-ThBA)–PVA hydrogel electrode, presenting the pseudocapacitive characteristics of the supercapacitor device. As a control, the CV of a device using bare CFC as electrodes was recorded, where a negligible capacitance could be observed (Fig. 5A). The CVs at different scan rates were measured, and the capacitances were calculated, as shown in Fig. 5B, while the typical GCD behaviour of the poly(EDOT-*co*-(Th-*g*-PAA)-*co*-ThBA)–PVA hydrogel-based device is shown in Fig. 5C. The specific capacitance of the device obtained by CV is 222.32 ± 7.59 mF cm^{-2} at a scan rate of 10 mV s^{-1} and that obtained by GCD is (218.75 ± 5.36) mF cm^{-2} at a current density of 0.2 mA cm^{-2}, with a maximum energy density of 19.8 μW h cm^{-2}. The obtained specific capacitance is remarkable when compared with reported conducting polymer-based flexible supercapacitors. A textile supercapacitor based on poly(3,4-ethylene dioxythiophene) polystyrene sulfonate (PEDOT:PSS) coated onto the cellulose/polyester cloth was reported, which provided a specific capacitance of 10 mF cm^{-2} at 1 mV s^{-1}.[35] A composite of PEDOT and graphene oxide (GO) was electrodeposited onto flexible electrode substrates in an ionic liquid (BMIMBF4) solution. The developed flexible supercapacitor exhibited an areal specific capacitance of 25 mF cm^{-2}.[36] A transparent, flexible supercapacitor was prepared from electrospun PEDOT:PSS nanofibers onto flexible polyethylene terephthalate (PET) substrates as electrodes for all solid-state supercapacitors, exhibiting a specific capacitance of 1.8 mF cm^{-2} at a discharging current of 5 μA cm^{-2}.[37] To satisfy the specific energy and power needs in applications, several supercapacitors were assembled either in series or in parallel to evaluate their performance for practical requirements, as shown in Fig. 5D. When the two supercapacitors were assembled in parallel, the discharge time was two times that of a single supercapacitor, at the same current density. When the two supercapacitors were connected in series, the supercapacitors demonstrated a 1.6 V charge/discharge voltage window with an equal discharge time, compared with the single supercapacitor.

The cycling stability is one of the most crucial characteristics of a supercapacitor device. The cycling stability of the poly(EDOT-*co*-(Th-*g*-PAA)-*co*-ThBA)–PVA hydrogel-based supercapacitor was evaluated by GCD testing at 10 mA cm^{-2} over the potential window between 0 and 0.8 V. The 95.8% of the capacitance was retained after 1000 charge–discharge cycles, as shown in Fig. 5E, while 89.6% of the areal specific capacitance was retained after 10 000 charge–discharge cycles (Fig. S4, ESI†). The first 5 cycles and the last 5 cycles are shown in the inset of Fig. 5E, demonstrating the stability and the retention of the long-term performance of the supercapacitor device. The capacitance retention (%) and EIS spectra of the poly(EDOT-*co*-(Th-*g*-PAA)-*co*-ThBA)–PVA hydrogel supercapacitor under flexing was investigated by GCD, where the device was bent at different

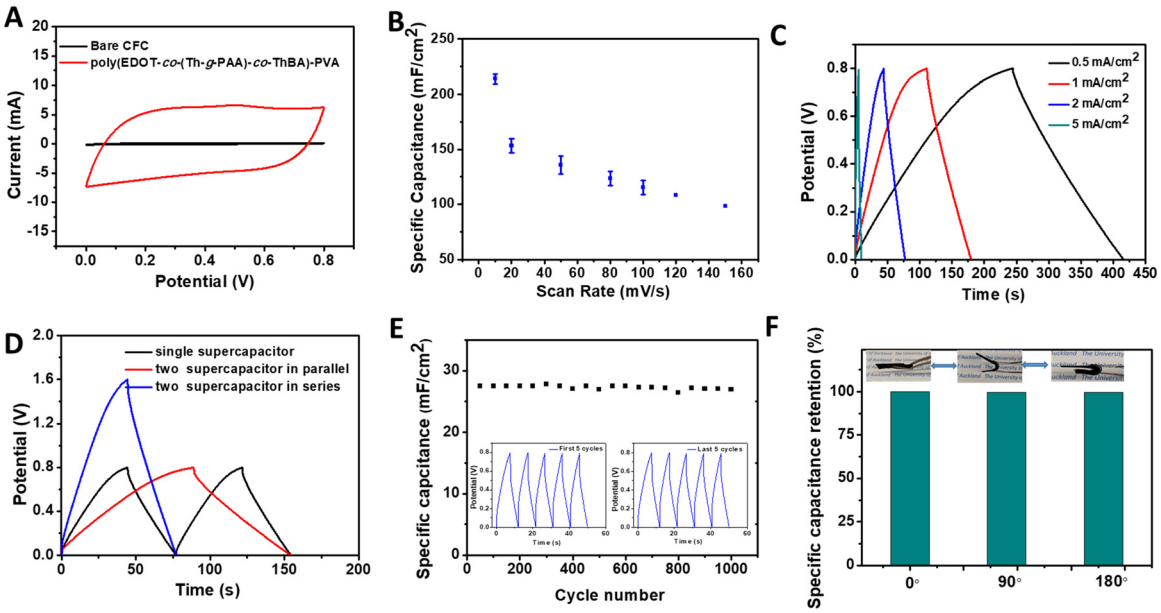

Fig. 5 (A) CV measurements of the flexible bare CFC and poly(EDOT-*co*-(Th-*g*-PAA)-*co*-ThBA)–PVA hydrogel-based supercapacitors at a scanning rate of 10 mV s^{-1}. (B) Specific capacitance plot of poly(EDOT-*co*-(Th-*g*-PAA)-*co*-ThBA)–PVA hydrogel-based supercapacitors at different scan rates. The error bars represent a standard deviation from 3 measurements. (C) GCD measurements of the supercapacitor device at various current densities. (D) GCD curves of a single supercapacitor, two supercapacitors connected in parallel, and two supercapacitors connected in series. (E) Specific capacitance obtained from GCD measurements with a current density of 10 mA cm^{-2} over 1000 charge–discharge cycles. Inset: the first five and the last five cycles of the GCD plots of the device. (F) Specific capacitance retention (%) of the device at different bending angles. Inset: the photographs showing the device after bending.

angles. As presented in Fig. 5F and Fig. S5 (ESI†), the areal capacitance and resistance remained practically the same under all bending conditions. The self-discharge test, in Fig. S6 (ESI†), reveals a fast self-discharge in the first 1 h, followed by a stable potential at 54% of the original potential in the following 6 h.

The self-healing properties (Fig. 6A inset) of the device were examined by CV measurements before and after healing, as shown in Fig. 6A. 78.3% of the specific capacitance remained after healing, calculated from CV measurements, which is comparable with the reported self-healing supercapacitor devices. Jin *et al.* reported a solid-state supercapacitor based on polyacrylic acid cross-linked by methacrylated graphene oxide (MGO–PAA) which showed a 60% recovery rate after cutting–healing cycles.[38] Ma *et al.* reported a self-healable PANI–PVA based hydrogel supercapacitor that retained 69% of the initial capacitance after the self-healing cycle,[39] where the healing property was from O–H–O hydrogen bonds between PVA polymer chains. In this work, the recovery of the specific capacitance for the device was improved by the presence of the self-healable hydrogel electrolyte, in comparison to the recovery rate of the poly(EDOT-*co*-(Th-*g*-PAA)-*co*-ThBA)–PVA hydrogel electrode. To demonstrate its self-healing ability, as shown in Fig. 6B, the two supercapacitors connected in series were able to light up a green LED after a cutting–healing cycle.

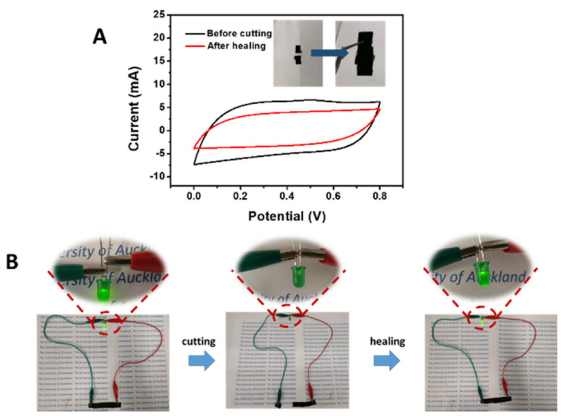

Fig. 6 (A) CV measurements of the device before cutting and after self-healing. Inset: The photographs showing the device before cutting and after healing. (B) The green LEDs were lighted up after a cutting–healing cycle.

Experimental

Materials

3,4-Ethylenedioxythiophene (EDOT), ammonium persulfate (APS), ferric trichloride ($FeCl_3$), thiophene-3-boronic acid (ThBA), potassium chloride (KCl), poly(4-styrenesulfonic acid) solution (PSS) (18 wt%) and poly(vinyl alcohol) (PVA, 99% hydration degree, M_w 146 000–186 000, were purchased from Sigma-Aldrich and used without further purification. Carbon fibre cloth (CFC) was purchased from Fuel Cell Store (USA).

Synthesis of the monomer 2-(thiophen-3-yl)ethyl 2-bromo-2-methylpropanoate (ThBr).

ThBr was prepared according to our previous report.[40] A solution of α-bromoisobutyryl bromide (BIB, 9.2 g, 40.0 mmol)

in DCM (12 mL) was added dropwise to a stirred solution of 3-thiopheneethanol (4.0 g, 31.2 mmol) and triethylamine (Et3N) (5.6 mL, 40.0 mmol) in pre-degassed DCM (28 mL) at 0 °C. The mixture solution was stirred for 30 min at room temperature for 24 h. The resultant mixture was diluted with DCM (40 mL) and filtered. The filtrate was then concentrated and washed with saturated sodium carbonate, brine solution and deionised water sequentially. The isolated organic layer was dried using $MgSO_4$, filtered, and concentrated. The product was purified by column chromatography on silica gel, with DCM as the eluent, to obtain ThBr as pale yellowish oil.

Grafting of poly(acrylic acid) to ThBr

Poly(acrylic acid) (PAA) side chains on ThBr were prepared by grafting *tert*-butyl acrylate (*t*BA) from ThBr by an activator regenerated by electron transfer–atom transfer radical polymerisation (ARGET–ATRP).[41] *t*BA (4.4 mL, 34.3 mmol), acetone (2.5 mL), $CuCl_2$ (1.2 mg, 82.3 nmol), PMDETA (65 μL, 0.3 mmol) and ThBr (780 mg, 2.3 mmol) were added to a 10 ml round bottom flask and degassed with nitrogen for 30 min. Tin(II)ethylhexanoate (0.3 mL, 0.9 mmol) as the reductant was then added and the mixture was quickly sealed, immersed in a preheated oil bath (60 °C) and stirred for 3 h. The reaction was stopped by exposing the mixture to air and cooled down to room temperature. After the reaction, the mixture solution was first passed through a column packed with activated neutral aluminium oxide, followed by precipitating in a cold MeOH/H_2O (70/30) (v/v) mixture, washing with MeOH twice, and drying under vacuum at room temperature.[42] The length of side chain was controlled by the mole ratio of *t*BA to ThBr, where the mole amount of ThBr was kept constant.

0.5 g of the obtained poly(*t*BA) grafted on ThBr (Th-*g*-poly(*t*BA)) was dissolved in 30 mL of the trifluoroacetic acid/chloroform mixture (30/70 v/v) and left overnight under stirring at room temperature.[43] After hydrolysis, the Th-*g*-PAA solution was concentrated using a rotary evaporator to afford a solid residue, which subsequently was washed several times with diethyl ether and dried under vacuum overnight at room temperature. The 1H NMR spectrum of the product in d6-DMSO indicated full hydrolysis of the *tert*-butyl ester groups (δ = 1.41 ppm, singlet, 9H) to acid groups as the new peaks appeared at δ = 12.2 (s, –COOH), 2.1–2.4 (C<u>H</u>–CH_2), and 1.5–1.9 (<u>CH_2</u>–CH). The length of the side PAA chain on (Th-*g*-PAA) was obtained from the ratio of integration of one of these peaks to the integrated peak at δ = 6.98 (s, thiophene).

Synthesis of the poly(EDOT-*co*-(Th-*g*-PAA)-*co*-ThBA)–PVA hydrogel

In a typical experiment, 270 μL of 10%wt PVA (in DMSO) solution was first mixed with 20 μL of poly(4-styrenesulfonic acid) solution (PSS) (18 wt%), named 'Solution A'. 4 μmol (Th-*g*-PAA) and 0.04 mmol thiophene-3-boronic acid (ThBA) were dissolved in 200 μL of DMSO and 0.8 mmol EDOT or thiophene monomer was added to the mixture, named 'Solution B'. After three monomers were fully dissolved, Solution B was added to Solution A under stirring, forming 'Solution C'.

For polymerisation, 0.16 mmol ammonium persulfate (APS) in 250 μL of deionised water was first added to Solution C under stirring at 60 °C, followed by the addition of 1.6 mmol $FeCl_3$ in 200 μL of water. The molar ratio of total monomers to Fe^{3+} to APS was 5 : 10 : 1. The mixture was kept at 60 °C for 12 h to complete the polymerisation. After polymerisation, the resultant poly(EDOT-*co*-(Th-*g*-PAA)-*co*-ThBA)–PVA hydrogels were washed thoroughly by immersing in distilled water for 24 h to remove the unreacted monomer and excess of ions.

Preparation of poly(EDOT-*co*-(Th-*g*-PAA)-*co*-ThBA)–PVA hydrogel electrodes

The carbon fibre cloth was immersed in 6 M HNO_3 (aq.) overnight, followed by washing with deionised water, ethanol and acetone and then dried in the oven at 60 °C. It was UV-ozone treated for 30 min before the use.[25] After the surface treatment, a hydrophilic carbon cloth with a water contact angle of 62.3° was obtained that was cut into rectangular shapes. The reaction mixture for the prepared poly(EDOT-*co*-(Th-*g*-PAA)-*co*-ThBA)–PVA hydrogel was cast onto the carbon cloth with a coating area of 1 cm × 1 cm and kept at 60 °C for 12 h. The poly(EDOT-*co*-(Th-*g*-PAA)-*co*-ThBA)–PVA hydrogel electrodes were washed thrice thoroughly by immersing in distilled water for 24 h.

Preparation of poly(EDOT-*co*-(Th-*g*-PAA)-*co*-ThBA)–PVA hydrogel-based flexible solid-state supercapacitors

The free-standing boron cross-linked PVA/KCl hydrogel electrolyte was prepared using a reported methodology.[26] 0.15 g PVA was dissolved in 0.75 mL of distilled water with stirring at 90 °C to form a transparent solution. The pH of the PVA solution was adjusted to pH 3 by 1 M HCl solution. 0.25 mL of KCl solution (3.0 mol L^{-1}) and 50 μL of borax solution (0.1 mol L^{-1}) were added slowly under stirring. Subsequently, the pH of the PVA/KCl mixture was adjusted to pH 9 by ammonia (25 wt%) to obtain a transparent PVA/KCl hydrogel electrolyte. The PVA/KCl hydrogel was assembled in between the two poly(EDOT-*co*-(Th-*g*-PAA)-*co*-ThBA)–PVA hydrogel electrodes, forming a sandwiched, flexible, hydrogel-based supercapacitor.

Electrochemical characterisation

Cyclic voltammogram (CV), galvanostatic charge/discharge (GCD) test and electrochemical impedance spectroscopy (EIS) measurement were carried out to test the electrochemical performance of the poly(EDOT-*co*-(Th-*g*-PAA)-*co*-ThBA)–PVA hydrogel. In a three-electrode cell, the electrolyte was 2 M KCl aqueous electrolyte, with platinum (Pt) and Ag/AgCl electrodes used as the counter electrode (CE) and reference electrode (RE), respectively. In CV measurements, the potential was scanned from 0 to 0.8 V (*vs.* Ag/AgCl RE), with a range of scan rates from 5 to 100 mV s^{-1}. EIS was performed in the frequency range of 0.01 Hz to 100 kHz at open circuit potential with an amplitude of 10 mV. GCD tests were carried out by scanning in the potential range of 0–0.8 V at different discharge current densities.

For the device, electrochemical measurements were performed on a two-electrode system, where the CV was recorded in the potential range of 0 to 0.8 V and GCD measurements by potential scanning from 0 to 0.8 V at different current densities.

Other characterisation

The scanning electron microscopy (SEM) of the dehydrated poly(EDOT-*co*-(Th-*g*-PAA)-*co*-ThBA)–PVA hydrogel was performed using a Philips XL30 SEM. FTIR spectra were recorded using an FTIR Bruker Vertex 70 spectrometer, with wavelength scanning from 4000 to 400 cm^{-1}. Raman measurements were performed using a LabRam HR Evolution confocal spectroscope (Horiba Japan) equipped with a 600 l mm^{-1} diffraction grating and an air-cooled CCD detector. Samples were excited using a 532 nm Nd:Yag laser passed through a 99% neutral density filter and focused through a 50× objective lens (Olympus, NA 0.5) for 90 s and 10 accumulations. X-Ray diffraction (XRD) analysis was performed using a PANalytical Empyrean X-ray diffractometer (45 kV, 40 mA) with Ni-filtered Cu Kα radiation.

Conclusions

A stretchable, soft, self-healable supramolecular conducting polymer-based hydrogel electrode is developed for use in flexible supercapacitor devices. A flexible supramolecular conducting polymer of poly(EDOT-*co*-(Th-*g*-PAA)-*co*-ThBA)–PVA was prepared by oxidative chemical polymerisation from three monomers: EDOT, PAA-grafted-thiophene and thiophene-3-boronic acid (ThBA). The boronic acid groups from ThBA provide self-assembly features through supramolecular interactions with hydroxyl groups from the soft PVA polymer. This supramolecular assembly enhances the mechanical and electrochemical properties of the hydrogel electrode. The self-healing properties were provided by the hydrogen bonds between carboxylic acid groups from the PAA-grafted thiophene and PVA. The composition of the poly(EDOT-*co*-(Th-*g*-PAA)-*co*-ThBA)–PVA hydrogel electrode was optimised in terms of the electrode capacitance, and the optimised electrode offered a combination of notable stretchability, fast self-healing and excellent electrochemical properties. These self-healable, stretchable hydrogel electrodes were integrated with the self-healable, soft PVA-based hydrogel electrolyte to obtain a supercapacitor device. The soft and flexible supercapacitor device exhibited a significant capacitance of (222.32 ± 7.59) mF cm^{-2} at a scan rate of 10 mV s^{-1}, an energy density of 19.8 μW h cm^{-2}, an excellent capacitance retention of about 95.8% after 1000 cycles, and a recovery rate of 78.3% after the cutting–healing cycle. The developed supramolecular conducting polymer hydrogel-based flexible and healable supercapacitor has great potential to be utilised as the flexible energy storage device for the next generation of epidermal bioelectronics devices.

Author contributions

Bicheng Zhu contributed to materials preparation, materials characterisation, and writing the original manuscript. Eddie Wai Chan synthesised 2-(thiophen-3-yl)ethyl 2-bromo-2-methylpropanoate (ThBr). Sheung Yin Li contributed to the ATRP grafting. Xin Sun contributed to the characterisation of the poly(EDOT-*co*-(Th-*g*-PAA)-*co*-ThBA)–PVA hydrogel. Jadranka Travas-Sejdic did the supervision, reviewing and editing.

Conflicts of interest

There are no conflicts to declare.

Acknowledgements

The authors would like to thank Science for Technological Innovation (SfTI) seed fund (UOAX2006) for financial support. The authors would like to thank Dr Cherie Tollemache for technical support and collection of the Raman Spectra.

References

1 Y. R. Jeong, G. Lee, H. Park and J. S. Ha, *Acc. Chem. Res.*, 2019, **52**, 91–99.
2 P. Baek, L. Voorhaar, D. Barker and J. Travas-Sejdic, *Acc. Chem. Res.*, 2018, **51**, 1581–1589.
3 A. M. Bryan, L. M. Santino, Y. Lu, S. Acharya and J. M. D'Arcy, *Chem. Mater.*, 2016, **28**, 5989–5998.
4 S. Sardana, A. Gupta, K. Singh, A. S. Maan and A. Ohlan, *J. Energy Storage*, 2022, **45**, 103510.
5 D. Zhao, Q. Zhang, W. Chen, X. Yi, S. Liu, Q. Wang, Y. Liu, J. Li, X. Li and H. Yu, *ACS Appl. Mater. Interfaces*, 2017, **9**, 13213–13222.
6 M. Wang, P. Baek, A. Akbarinejad, D. Barker and J. Travas-Sejdic, *J. Mater. Chem. C*, 2019, **7**, 5534–5552.
7 X. Wang, J. Zhou, Y. Zhu, W. Cheng, D. Zhao, G. Xu and H. Yu, *Chem. Eng. J.*, 2020, **392**, 123644.
8 D. Zhao, Y. Zhu, W. Cheng, G. Xu, Q. Wang, S. Liu, J. Li, C. Chen, H. Yu and L. Hu, *Matter*, 2020, **2**, 390–403.
9 M. Huang, Y. Hou, Y. Li, D. Wang and L. Zhang, *Des. Monomers Polym.*, 2017, **20**, 505–513.
10 K. Wang, X. Zhang, C. Li, X. Sun, Q. Meng, Y. Ma and Z. Wei, *Adv. Mater.*, 2015, **27**, 7451–7457.
11 K. Sun, E. Feng, G. Zhao, H. Peng, G. Wei, Y. Lv and G. Ma, *ACS Sustainable Chem. Eng.*, 2019, **7**, 165–173.
12 J. Li, W. Yan, G. Zhang, R. Sun and D. Ho, *Mater. Chem. C*, 2021, **9**, 1685–1692.
13 H. Lu, Y. Li, Q. Chen, L. Chen, N. Zhang and M. Ma, *ACS Appl. Energy Mater.*, 2019, **2**, 8163–8172.
14 W. Li, F. Gao, X. Wang, N. Zhang and M. Ma, *Angew. Chem., Int. Ed.*, 2016, **128**, 9342–9347.
15 Q. Chen, H. Lu, F. Chen, L. Chen, N. Zhang and M. Ma, *ACS Appl. Energy Mater.*, 2018, **1**, 4261–4268.
16 J. J. Alcaraz-Espinoza, G. Ramos-Sánchez, J. H. Sierra-Uribe and I. González, *ACS Appl. Energy Mater.*, 2021, **4**, 9099–9110.
17 M. C. G. Saborío, S. Lanzalaco, G. Fabregat, J. Puiggalí, F. Estrany and C. Alemán, *J. Phys. Chem. C*, 2018, **122**, 1078–1090.

18 J. Kang, J. B. H. Tok and Z. Bao, *Nat. Electron.*, 2019, **2**, 144–150.
19 Y. Huang, M. Zhong, Y. Huang, M. Zhu, Z. Pei, Z. Wang, Q. Xue, X. Xie and C. Zhi, *Nat. Commun.*, 2015, **6**, 10310.
20 J. Han, H. Wang, Y. Yue, C. Mei, J. Chen, C. Huang, Q. Wu and X. Xu, *Carbon*, 2019, **149**, 1–18.
21 J. Yang, X. Yu, X. Sun, Q. Kang, L. Zhu, G. Qin, A. Zhou, G. Sun and Q. Chen, *ACS Appl. Mater. Interfaces*, 2020, **12**, 9736–9745.
22 Y. Guan and Y. Zhang, *Chem. Soc. Rev.*, 2013, **42**, 8106–8121.
23 S. Lee and C. H. Park, *Text. Res. J.*, 2019, **89**, 2376–2394.
24 H. Wei, M. Lei, P. Zhang, J. Leng, Z. Zheng and Y. Yu, *Nat. Commun.*, 2021, **12**, 2082.
25 H. Yu, N. Rouelle, A. Qiu, J.-A. Oh, D. M. Kempaiah, J. D. Whittle, M. Aakyiir, W. Xing and J. Ma, *ACS Appl. Mater. Interfaces*, 2020, **12**, 37977–37985.
26 Q. Liu, J. Qiu, C. Yang, L. Zang, G. Zhang and E. Sakai, *Adv. Mater. Technol.*, 2021, **6**, 2000919.
27 Y.-N. Chen, C. Jiao, Y. Zhao, J. Zhang and H. Wang, *ACS Omega*, 2018, **3**, 11788–11795.
28 H.-R. Lim, H. S. Kim, R. Qazi, Y.-T. Kwon, J.-W. Jeong and W.-H. Yeo, *E&E*, 2020, **32**, 1901924.
29 Y. Zou, C. Chen, Y. Sun, S. Gan, L. Dong, J. Zhao and J. Rong, *Chem. Eng. J.*, 2021, **418**, 128616.
30 H.-H. Chang, C.-K. Chang, Y.-C. Tsai and C.-S. Liao, *Carbon*, 2012, **50**, 2331–2336.
31 Z. Al-Ghaus, A. Akbarinejad, B. Zhu and J. Travas-Sejdic, *J. Mater. Chem. A*, 2021, **9**, 20783–20793.
32 H. Zhou, G. Han, Y. Xiao, Y. Chang and H.-J. Zhai, *J. Power Sources*, 2014, **263**, 259–267.
33 Z. Wang and Q. Pan, *Adv. Funct. Mater.*, 2017, **27**, 1700690.
34 H. Peng, Y. Lv, G. Wei, J. Zhou, X. Gao, K. Sun, G. Ma and Z. Lei, *J. Power Sources*, 2019, **431**, 210–219.
35 L. Manjakkal, A. Pullanchiyodan, N. Yogeswaran, E. S. Hosseini and R. Dahiya, *Adv. Mater.*, 2020, **32**, 1907254.
36 S. Lehtimäki, M. Suominen, P. Damlin, S. Tuukkanen, C. Kvarnström and D. Lupo, *ACS Appl. Mater. Interfaces*, 2015, **7**, 22137–22147.
37 J. Cárdenas-Martínez, B. L. España-Sánchez, R. Esparza and J. A. Ávila-Niño, *Synth. Met.*, 2020, **267**, 116436.
38 X. Jin, G. Sun, H. Yang, G. Zhang, Y. Xiao, J. Gao, Z. Zhang and L. Qu, *J. Mater. Chem. A*, 2018, **6**, 19463–19469.
39 W.-B. Ma, K.-H. Zhu, S.-F. Ye, Y. Wang, L. Guo, X.-Y. Tao, L.-T. Guo, H.-L. Fan, Z.-S. Liu, Y.-B. Zhu and X.-Y. Wei, *Mater. Sci.: Mater. Electron.*, 2021, **32**, 20445–20460.
40 M. Wang, S. Kee, P. Baek, M. S. Ting, Z. Zujovic, D. Barker and J. Travas-Sejdic, *Polym. Chem.*, 2019, **10**, 6278–6289.
41 T. E. Kerr-Phillips, N. Aydemir, E. W. C. Chan, D. Barker, J. Malmström, C. Plesse and J. Travas-Sejdic, *Biosens. Bioelectron.*, 2018, **100**, 549–555.
42 A. de Cuendias, M. Le Hellaye, S. Lecommandoux, E. Cloutet and H. Cramail, *J. Mater. Chem.*, 2005, **15**, 3264–3267.
43 E. Hasan, S. Furzeland, D. Atkins, D. J. Adams and J. V. M. Weaver, *Polym. Chem.*, 2012, **3**, 625–627.